POLITECNICO DI TORINO
Repository ISTITUZIONALE

A "Plant-Wearable System" for Its Health Monitoring by Intra- and Interplant Communication

(Article begins on next page)

27 April 2024

A "plant-wearable system" for its health monitoring by intra- and inter-plant communication

Umberto Garlando, *Member, IEEE,* Stefano Calvo, *Student Member, IEEE,,* Mattia Barezzi, *Student Member, IEEE,* Alessandro Sanginario, *Member, IEEE,*
Paolo Motto Ros, *Member, IEEE,* and Danilo Demarchi, *Senior Member, IEEE*

Abstract—A step forward in smart agriculture is moving to direct monitoring plants and crops instead of their environment. Understanding plant status is crucial in improving food production and reducing the usage of water and chemicals in agriculture.

Here we propose a "plant-wearable", low-cost, and low-power method to measure in-vivo green plant stem frequency as the indicator for plant watering stress status. Our method is based on measuring the frequency of a digital signal obtained with a relaxation oscillator where the plant is part of the feedback loop. The frequency was correlated with the soil water potential, used as a critical indicator of plant water stress, and an 85% correlation was found. In this way, the measuring system matches all the requirements of smart agriculture and IoT: ultra-low-cost, low-complexity, ultra-low-power, and small sizes, introducing the concept of wearability in plant monitoring. The proposed solution exploits the plant and the soil as a communication channel: the signal carrying the plant watering stress status information is transmitted to a receiving system connected to a different plant. The system's current consumption is lower than $50\mu A$ during the transmission in the plant and 40mA for wireless communication. During inactivity periods, the total current consumption is lower than $15\mu A$.

Another important aspect is that the system has to be energy autonomous. Our proposal is based on energy harvesting solutions from multiple sources: solar cells and plant microbial fuel cells. This way, the system is battery-less thanks to supercapacitors as a storage element. The system can be deployed in the fields and used to monitor plants directly in their environment.

Index Terms—Smart Agriculture, in-vivo monitoring, impedance monitoring, water stress, intra-plant commununication

I. INTRODUCTION

CLIMATE change and urbanization are two of the leading causes of arable land reduction. Authors in [1] found that over 5 million square kilometers of drylands have already turned into deserts because of human activities. Climate change and the reduction of soil quality [2] will have a major impact on food production [3].

Food production has a massive impact on the climate. It contributes to one-fourth of the global amount of greenhouse gas emission [4], and its impact is destined to grow since the world's population is expected to reach 10 billion within this century [5]. Therefore, a novel approach to food production is needed to ensure sustainability and security both from the point of view of health and quantity.

U. Garlando, S. Calvo, M. Barezzi, A. Sanginario, P. Motto Ros and D. Demarchi are with the Department of Electronics and Telecommunications, Politecnico di Torino, Torino, Italy.
Corresponding author: umberto.garlando@polito.it

Smart agriculture combines engineering and farming knowledge to achieve these two goals.

Environment analysis is the most common method applied in smart agriculture, but it is not the most efficient. Authors in [6] and [7] present the application of weather station to monitor the environment surrounding the crops to perform weather forecasts, while Nakayama et al. infer information regarding soil water content exploiting an infra-red light source [8]. Inferring crops' health status by analyzing their environment could be misleading. Garlando et al. showed that environmental sensors might not be sufficient to understand crops' health status [9]

Thus, sensors directly implemented on crops have been developed to inspect key parameters to extract information about their health status. Sensors applied directly onto the crops have been implemented in wireless sensor networks to gather information regarding leaf temperature [10] and wetness [11], stomata transpiration [12], leaves water content [13], and leaves and stem growth rate [14], [15]. Crops' water stress status is a key parameter to properly manage crop irrigation. This parameter has been inspected by reading the electrical potential that develops between crops' stems and the substrate where they are growing [16]. Another useful parameter to asses information regarding this kind of stress is the stem electrical impedance. Although the two methods assess information on the same parameter, they can not be compared since they rely on monitoring two different physical quantities. It has been found that stem electrical impedance varies when the plant is subjected to particular stimuli. It could detect plants' watering stress issues that environmental analysis may not [9], [17], [18].

Studies regarding soil and plant stems and trunks highlight that they can be used as communication channels in which an electric signal can propagate [19], [20]. These papers show that soil is electrically conductive (and, thus, may be exploited to propagate a signal) and that transferring bits through plants' trunks is possible.

The work presented in this paper is grafted on these three latter discoveries (soil electrical conductivity, trunk's conductivity, and environmental sensors inaccuracy). It deals with a novel approach to inspect in-vivo and real time plant stem frequency and, at the same time, it aims at paving the way to the development of the concept of the Internet of Plants (IoP).

Besides intra-body communication, presented by Motto Ros et al. in [20], we demonstrated that plants could communicate with each other through the soil. Therefore, stem frequency

evaluation has been performed by reading the signal injected into a tobacco plant from another one. As the Results and Discussion section explains, this signal frequency strictly correlates to the stem impedance. Therefore, it can be exploited to gather information regarding plant watering stress status.

A key aspect of smart agriculture devices is power consumption. The system presented here is energy autonomous since it exploits energy harvesting from different sources.

Given the proposed system's simplicity and efficiency, it can be deployed on the field without needing batteries.

Every experiment carried out and presented in the following has been performed with tobacco plants (*Nicotiana Tabacum*). Each plant was about $60\,cm$ high, grown indoors, and subjected to water stress.

In this paper, we prove that the stem frequency is a valid parameter to monitor the plant water stress since it is highly correlated to the electrical impedance and is propagated in the plant itself, giving the possibility to read this information from neighboring plants.

Moreover, low-power consumption, system simplicity, and inter-plants communication may provide the possibility to install a sufficiently high number of sensing systems (nodes) to reach a high level of capillarity into the fields. Inter-plants communication would allow for the installation of multiple sensing nodes sending their data to a single receiving node without relying on RF communication protocols. This would reduce the overall power consumption increasing the system life span and reliability.

The paper is organized as follows: section II describes the designed circuit and how the experiments were performed. Section III shows the results, and conclusions are described in section IV.

II. PROPOSED DESIGN AND METHODS

In-vivo stem impedance measurements carried until now rely on complex, time-consuming, and expensive systems [9], [17]. This approach is not feasible if the analysis is meant to be performed in a field. Thus, to overcome this limit, we decided to inspect an oscillating signal frequency (stem frequency) generated by an integrated circuit having a portion of the plant stem in its feedback loop.

This choice has been made since an electric signal frequency can be easily monitored nowadays with a cheap, small, and low-power embedded system equipped with a Micro-Controller Unit (MCU) performing a digital measurement. We also soon see the possibility of exploiting flexible and biodegradable electronics for implementing the solution we are presenting.

A. Impedance and Frequency Correlation for Plant Health Monitoring

The first step towards feasible in-vivo and in-situ stem frequency monitoring demonstrated a strong correlation between stem electrical impedance and stem frequency. This task was achieved by analyzing both stem electrical impedance and frequency simultaneously, thanks to a relay-based system and two bench instruments. Together with stem electrical impedance and frequency, the soil water potential (SWP), ambient light, air humidity, and temperature were measured. SWP is strictly related to soil moisture and plants' watering stress status [21], [22]. It estimates a plant's effort to absorb water from the soil. Therefore, it takes into account both water concentration and soil texture. Correlation among stem frequency, electrical impedance, and soil water potential was inspected by exploiting a custom PCB [17] mounted on a RaspBerry pi Zero. This board was used both to monitor SWP variations and to provide power to a Texas Instruments LMC555 timer mounted on a bread-board with a portion of a tobacco plant stem with a length of about $5\,cm$ in its feedback loop. SWP was monitored thanks to an Irrometer Watermark sensor made of a piece of porous gypsum in contact with the surrounding soil. This is a resistive sensor: gypsum electrical resistance depends on the water content of the surrounding media. Stem impedance, SWP, and stem frequency were sampled once per hour.

Impedances were measured with a bench impedance meter (HP Agilent, 4294A) exploiting a 4-probes measurement method [23] performing impedance spectroscopy. Stem frequencies and SWP were read by a bench frequency counter (HP Agilent, 53181A). Temperature and humidity were measured with a Texas Instruments HDC2080, while light intensity with a Texas Instruments OPT3001. These devices were read by the RaspBerry pi Zero through an I2C interface.

Other important parameters (such as soil salinity) that may affect plants' health status were not considered to keep the measuring system simple.

B. Intra- and Inter-Plant Communication

Plant's leaves, branches, roots, and stem exchange substances. Thus, this process involves the entire plant and occurs through channels crossing the whole plant (xylem and phloem) [24]. A recent study showed that these tissues are electrically conductive [25]. This means that an electrical signal injected into the stem can propagate along it and be collected on a different point of the stem [20].

Soil is electrically conductive too [26], [27]. Therefore, it can be exploited to propagate an electrical signal from one plant to another.

Thus, stem and soil conductivity may be exploited for stem frequency analysis and SWP monitoring.

Two systems were designed to perform this experiment. The first is a transmitting system whose task is to generate the signal carrying the stem frequency and inject it into the plant's stem under test. Similarly to the experiment previously described, the transmitter was equipped with a relaxation oscillator (LMC555) with a portion of the plant stem in its feedback loop. Therefore, the stem frequency was related to the stem electrical impedance.

The second is a receiver designed to read this frequency and execute SWP monitoring by exploiting the device described in the previous section. These two systems were placed on two plants growing in the same pot and about $20\,cm$ far from each other. Therefore, plants did not directly touch. The signal with the information related to stem frequency traveled inside the
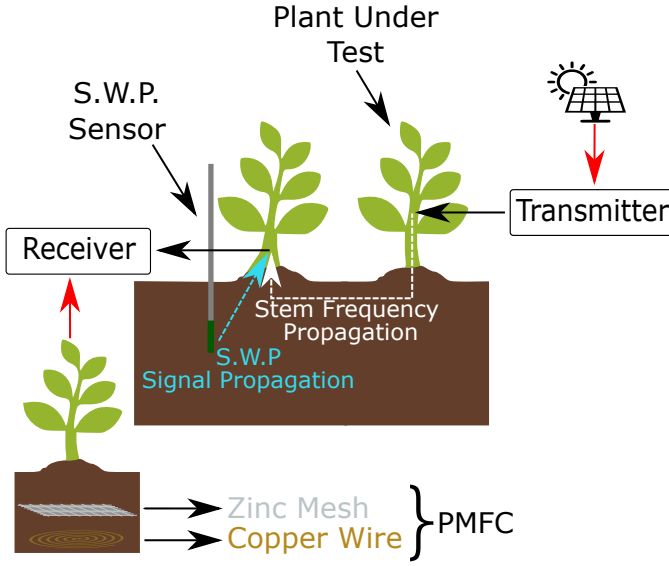
Fig. 1. Experimental setup schematics. The dashed white line highlights the path that the signal carrying the stem frequency followed, while the light blue one refers to the signal carrying the SWP information followed.

stem plant under test, its roots, the soil, and the other plant (where the receiver system was placed). The signal carrying the information related to SWP level was injected into the soil by the Watermark sensor (electrically in contact with the soil); it traveled through the soil, the plant where the receiving system was placed, and this device read it.

The experimental set-up and the paths followed by the analyzed signals are reported in figure 1. Since this analysis is meant to be performed in a field, the system must not rely on power grids.

For this reason, a completely autonomous system (relying on small poly-crystalline silicon solar cells) injecting the stem frequency inside the plant under test was placed on its stem (about $20\,\mathrm{cm}$ above the soil). In contrast, the receiving one, placed about $5\,\mathrm{cm}$ above the soil, was powered by a plant microbial fuel cell [28], [29]. The transmitting and the receiving systems were placed on the plants by piercing them with stainless steel needles (used as electrodes to connect the two systems to the two plants) with a diameter equal to $0.4\,\mathrm{mm}$. These needles' characteristics (thickness and material) provided good biocompatibility and resistance to deterioration. Experiments lasted several months without showing a significant impact on the results. Since the two systems were placed on two different plants, they did not share the reference voltage (ground). The receiving system's purpose was evaluating the stem frequency and SWP level, storing their values, and sending them to a base unit through *LoRa* (Long Range) radio-frequency communication protocol [30]. *LoRa* enables the deployment in the fields where internet access is unavailable, keeping very low power consumption. The transmitting (TX) and receiving systems (RX, described in the following) schematics are depicted in figure 2.a and 2.b respectively.

They are composed of off-the-shelf integrated circuits mounted on a custom PCB or a breadboard. Since both must
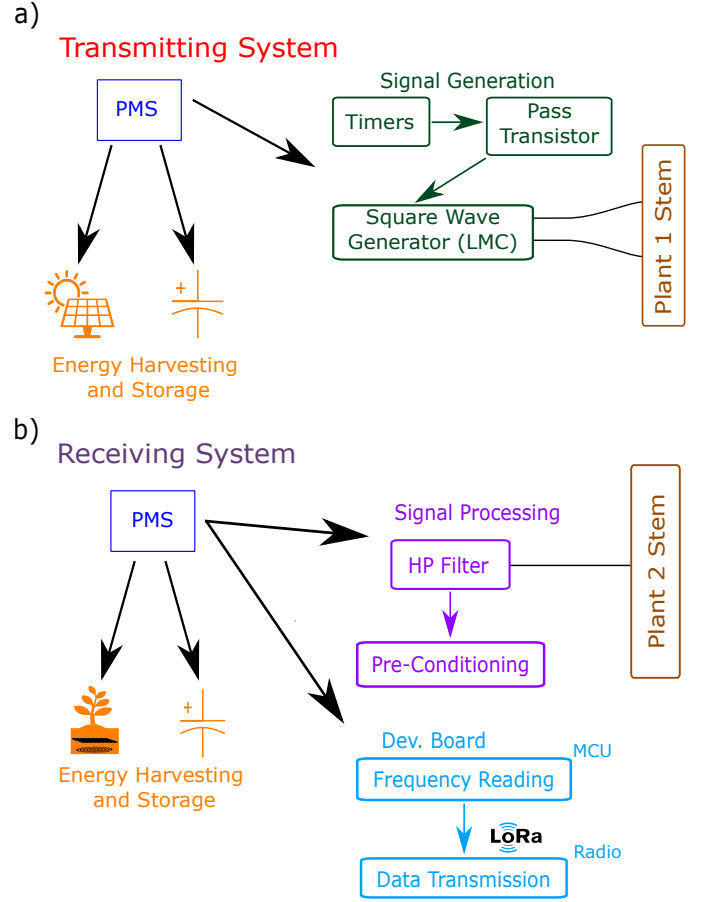

Fig. 2. a) Transmitting System schematics. The same color has been used to group devices that compose functioning blocks. b) Receiving System schematics. The same color has been used to group devices that compose functioning blocks.

be energetically autonomous and reliable, they were equipped with energy harvesting and storing devices. The transmitting system is powered by two small poly-crystalline based silicon solar cellsconnected to a Texas Instruments BQ25570EVM-206 (Power Management System, PMS) board. Further details regarding the solar cells are given at the end of this section. The energy storage device is a supercapacitor (PM-5R0V105-R) with a $1\,\mathrm{F}$ capacitance connected to the PMS. The power management system's purposes were to optimize the power coming from the solar cells (SCs), regulate the voltage on the storage element, and provide a regulated output voltage to the rest of the transmitting system. The first purpose is achieved by sampling the solar cells (SC) open circuit voltage (V_{oc}) once every $16\,\mathrm{s}$ and regulating the PMS input impedance to set the SCs' operating voltage equal to 80% of V_{oc}. As it is widely known, solar cells' output power maximizes when their operating voltage is around 75-85% of their open circuit voltage. Storage device's voltage regulation and monitoring are performed to avoid excessively stressing the device and prevent the discharge under a level that may damage it. The PMS regulated output voltage was set to $1.8\,\mathrm{V}$. It was used to provide power to the rest of the transmitter composed of two Texas Instruments TPL5110 timers (used to perform only a few measurements per hour), one pass transistor (switch)
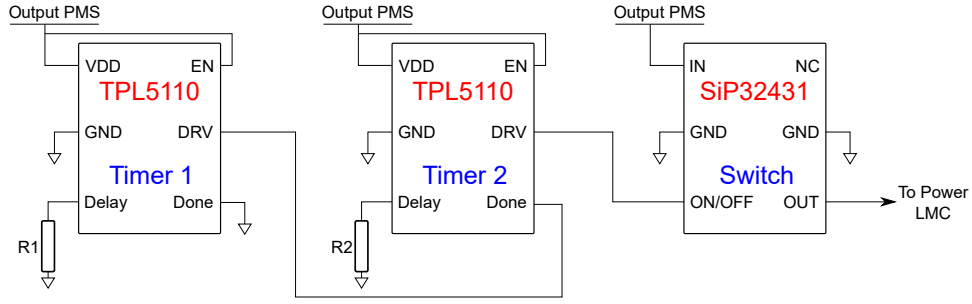
Fig. 3. Portion of transmitting system dedicated to measurement timing. Timer 1 is set to have a period of $3\,\mathrm{s}$ since R1 is a $7.6\,\mathrm{k\Omega}$ resistor, timer 2 has a $28\,\mathrm{min}$ period since R2 is a $82\,\mathrm{k\Omega}$ resistor. The switch output is connected to the LMC555 power pin.

Vishay SiP32431, and one Texas Instruments LMC555 timer used as a relaxation oscillator (square wave generator).

The two TPL timers were connected in a loop-like manner since the DRV pin of timer 1 was short-circuited to the DONE pin of the other. This configuration allowed us to set measurement duration (a few seconds) and system duty cycle (two measurements per hour). This goal was achieved since the two timers were used to pilot the pass transistor implemented to gate the PMS output power to the LMC555 responsible for the stem frequency generation. The two TPL timers and the pass transistor are directly connected to the PMS output, while the LMC timer is powered only when the pass transistor is active. TPL timers 1 and 2 work in the enable state, and their period is chosen to be equal to $3\,\mathrm{s}$ and $28\,\mathrm{min}$, respectively. Timer 1 DRV (output) pin is connected to timer 2 DONE pin, while this latter's DRV is connected to the pass transistor control pin. The switch's output is connected to the LMC555 supply pin.

Timers and pass transistor connection schematic is depicted in figure 3. Thanks to this configuration, it has been possible to perform one stem frequency evaluation lasting $3\,\mathrm{s}$ every $28\,\mathrm{min}$ without using an MCU for timing purposes, achieving very low power consumption. When the timing circuit is powered, both TPLs DRV pins are pulled down. Therefore, the pass transistor is turned on, providing power to the relaxation oscillator that injects the signal carrying the stem frequency into the plant under test. After 3 seconds, the timer 1 DRV pin goes up due to the timer configuration. This causes the timer 2 DRV to be pulled up since its Done pin will have a low-to-high transition. Therefore, the pass transistor control pin is pulled up, turning off the device and interrupting the energy supply to the LMC555. This measurement routine repeats when timer 2's period ends (28 minutes). The whole transmitting system current consumption was around $50\,\mathrm{\mu A}$ during measurements and less than $1\,\mathrm{\mu A}$ between two consecutive measurements.

The timing diagram related to measurement occurrences and the switch's control signal is reported in figure 4.

The LMC555 (square wave generator) was kept in the configuration used to obtain a $50\,\%$ duty cycle square wave as output with a frequency higher than $10\,\mathrm{kHz}$ to be correctly read by the receiver equipped with a high-pass filter.

The receiving system (RX) is powered by a plant microbial fuel cell (PMFC). Further details regarding PMFC's implementation and performances are given at the end of this
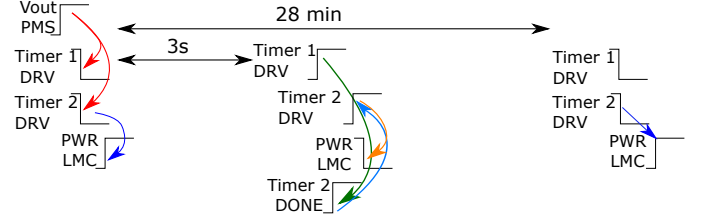

Fig. 4. Measurement timing diagram. Arrows highlight established cause-effect relationships that hold among signals.

section. Energy harvesting device, energy storage unit, and the rest of the RX were connected to a Texas Instruments BQ25570EVM-206 (Power Management System, PMS). This device was modified to provide a regulated output voltage equal to $3.3\,\mathrm{V}$. The device providing energy storage is a supercapacitor (PM-5R0V105-R) with a $1\,\mathrm{F}$ capacitance. The receiver is composed of two blocks. The first is a conditioning circuit with a passive first-order filter and a threshold voltage comparator. This circuitry filters the signal carrying the stem frequency and restores its digital behavior. The second block, a Micro-Controller Unit (MCU), reads the stem frequency and SWP level, saves them, and sends their values through *LoRa* protocol. The signal conditioning system's purposes are to filter out low-frequency (typically $50\,\mathrm{Hz}$ and its higher harmonics due to the European power grid) superimposed to the collected signal and to restore the signal in the digital domain. This latter conditioning was necessary since the stem frequency reading performed by the MCU was completely digital. This choice allowed us to avoid using the MCU analog peripherals that would increase its power consumption and are very sensitive to power voltage oscillations. This component is always present and hardly manageable in outdoor conditions. Therefore, the filter was designed to have a cut-off frequency equal to $10\,\mathrm{kHz}$. Thus, more than two orders of magnitude higher than the fundamental noise frequency coming from the power grid. The threshold comparator is made by an inverting rail-to-rail threshold comparator (Texas Instrument TLV7011) with $300\,\mathrm{mV}$ hysteresis. Hysteresis value was set to fit the experimental condition. This value may not be suited when, for example, soil dries even further, and its conductivity decreases. This would increase signal attenuation while traveling through the soil, leading to a received signal amplitude smaller than $300\,\mathrm{mV}$. This attenuation could be considered by dynamically
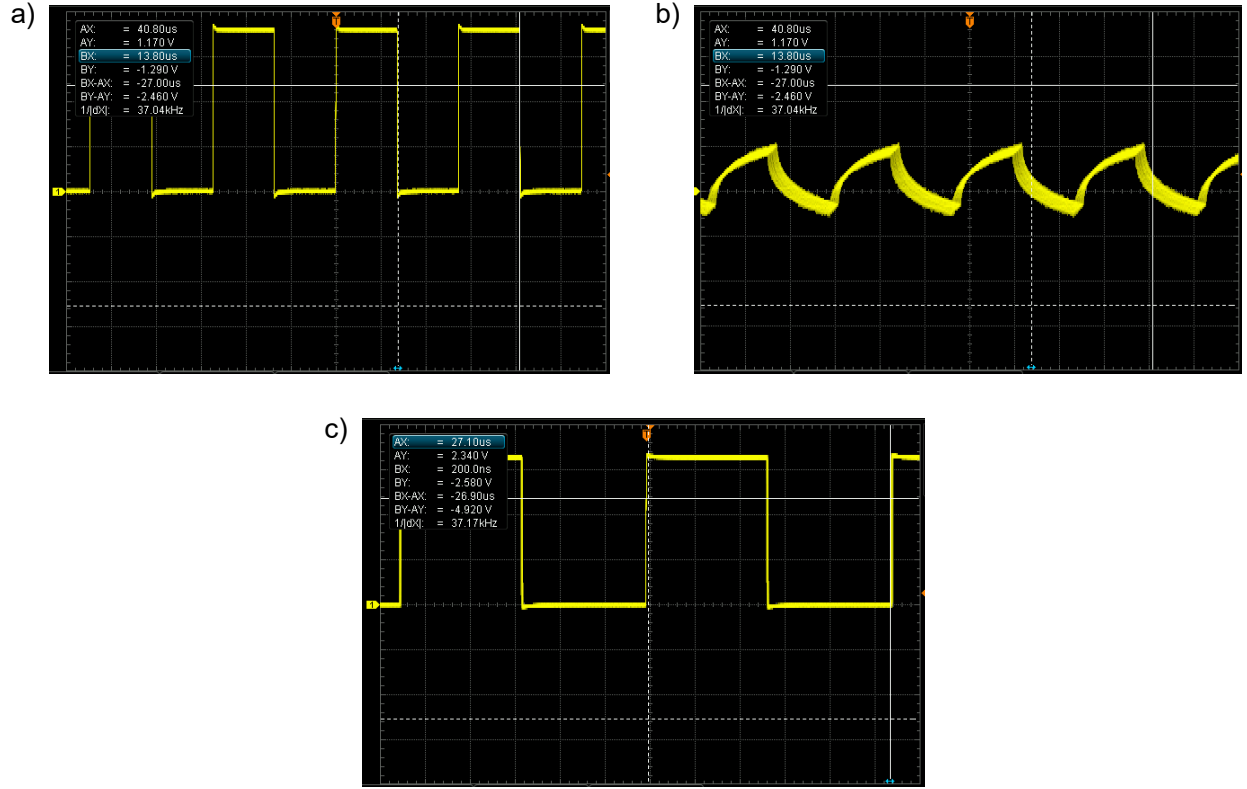
Fig. 5. Signal inspected with an oscilloscope. a) Signal generated by the TX and injected into the plant under test. b) Signal received by the RX before being conditioned by the high-pass filter. It can be seen that there is a noise superimposed on the correct signal (in fact, the line is thicker than the two other plots). c) Signal after the manipulation performed by the high-pass filter and the threshold voltage comparator. This signal is fed to the MCU. The 0.35% error present in the frequency of the reconstructed signal is due to cursor placement. It was impossible to acquire all these signals simultaneously since the interaction between the oscilloscope probe and the circuitry would change its behavior and would not allow the condition circuit to work properly.

changing the hysteresis value since the TLV7011 allows for easy thresholds tuning. Threshold comparator's duty was to convert the analog signal coming from the filter to a digital one between $0\,V$ and $3.3\,V$ that the MCU could read. Together with filtering low-frequencies, the filter also sets the signal's average value (DC component) at the midpoint of the threshold comparator input common-mode range. Since the transmitter and the receiver did not share the reference voltage, this was necessary to set the received signal values' reference to the receiver one, thus to its ground. This enabled the rest of the receiver to manage and read the signal properly. An example of the injected and received signal is shown in figure5.

Figure 6.a schematized the signal conditioning path. The RX's second block is a NUCLEO-STM32WL55JC1 development board equipped with an STM32WL55JC MCU. It is connected to the threshold comparator output, and it has to read the signal frequency (generated by the transmitter), store its value, evaluate the average between two consecutive measurements, and send it through *LoRa* protocol once per hour to a gateway (base unit) that made data accessible. The MCU was kept in low-power modes between two consecutive measurements. Moreover, a digital filter has been implemented in the code running on the MCU to further reduce the overall power consumption. Commutations performed by the threshold comparator output awakened the MCU from its low-power states. Then, the micro-controller checked if the

acquired frequency (due to TLV7011 commutations) was in the expected range. If the read frequency was not in this range, the MCU returned to its low-power state. Otherwise, the measurement procedure (stem frequency reading, storage, and transmission) continued. This digital filter improved noise and power management. Furthermore, the micro-controller performs the reading procedure of the watermark sensor. The signal injected in the watermark travels through soil, roots, and stem and is read through the same pin used to read the stem frequency. The whole receiving system current consumption was around $5\,mA$ while measurements occurred with a peak of about $35\,mA$ that lasted for a few ms for data transmission with the *LoRa* communication protocol. Between two consecutive measurements, the MCU was set to a low-power mode that allowed a total receiving system current consumption of around $15\,\mu A$.

Energy Harvesting Devices: The devices used to power the receiving and transmitting systems harvest energy from light and micro-biological activity in the soil close to the plant's roots, respectively. Two small poly-crystalline (around $6\,cm^2$ each) solar cells provided power to the transmitting system. Experiments took place in an indoor environment. Therefore, cell performances (voltage vs. current) have been measured with the impinging light coming from a lamp. Since the two cells were equivalent, only one has been characterized. Characterization was performed by connecting the cell to
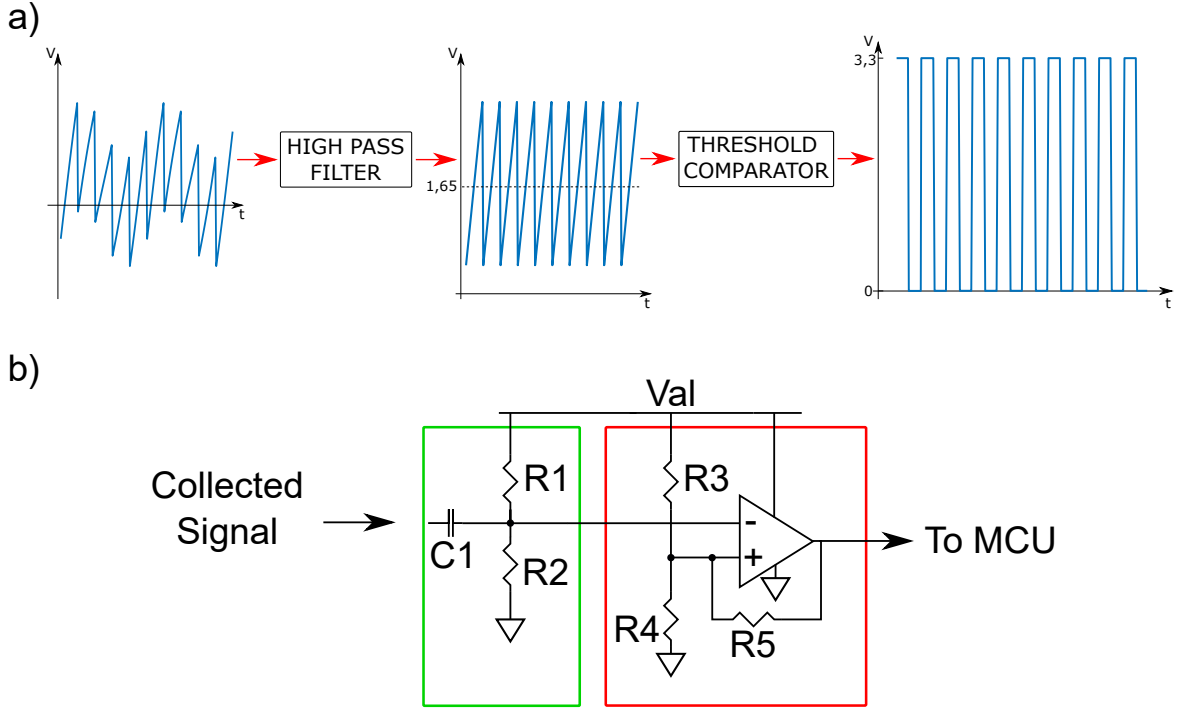
a)

b)

Fig. 6. a) Signal conditioning circuit schematized behavior. Signal behavior before and after each circuit block has been reported. As highlighted, the signal has an unknown average value before the first stage because of TX and RX electrical independence. Moreover, noise at low frequency is superimposed. The high-passing filter blocked the noise with the unknown signal bias point and restored a known one. This latter was chosen to be equal to the comparator's thresholds average values, $1.65\,\mathrm{V}$ (value chosen to be at the threshold comparator's input dynamics middle point). The threshold comparator output was a square wave with the same frequency as the original signal. Therefore, a GPIO input pin of any MCU could easily and correctly read it. b) Signal conditioning circuit schematics. Components encapsulated into the green rectangle form the high-pass filter collecting the signal from the plant. The ones encapsulated in the red rectangle form the threshold voltage comparator, whose output is directly fed to the MCU. V_{al} is the output power provided by the PMS equal to $3.3\,\mathrm{V}$.

a resistive load ranging from $10\,\Omega$ to $1\,\mathrm{M}\Omega$ and reading the voltage across the resistance with the Agilent 34401A bench multimeter. Results are shown in figure7. Performances clearly show that the combination of two cells connected in parallel provides enough energy for the system to work properly. Moreover, it is sufficient to keep the supercapacitor charged enough to ensure that the transmitter injects the signal for a few days even if the cells stop providing power. The receiving system (RX) is powered by a plant microbial fuel cell. The cell is composed of two electrodes placed inside the soil about $20\,\mathrm{cm}$ under the surface and with a relative distance of $5\,\mathrm{cm}$. The two electrodes were made of a zinc mesh and a copper wire shaped as a spiral [29]. The soil in which plants grow is composed of a mixture of sand, peat, manure, and ground leaves. The soil where plants grow is rich in microbes. Therefore, their biological activity can be exploited to extract electrical power [28] and provide it to the receiving system. PMFC's performances have been evaluated with the same method exploited to characterize the solar cell. Results presented in figure 8 show that it is suited to provide energy to the receiving system ensuring a satisfactory supercapacitor charging level. Due to PMFC electrodes material, performances may deteriorate in the long-term, but this did not happen during the experiments. The cell output power kept a satisfactory level.
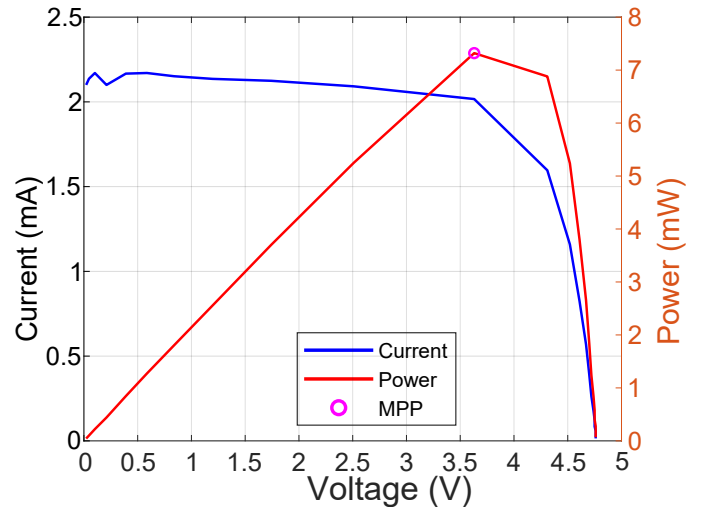

Fig. 7. The blue line is the cell's voltage vs. current characteristic, the red one represents the output power ($V \cdot I$) provided by th cell. The purple circle highlights the maximum power point (MPP) showing that it is approximately 80% of the open circuit voltage.

III. RESULTS AND DISCUSSION

A. Impedance and Frequency Correlation for Plant Health Monitoring

A recent study [17] showed that stem impedance is prone to noisy behaviors at lower frequencies. The same research
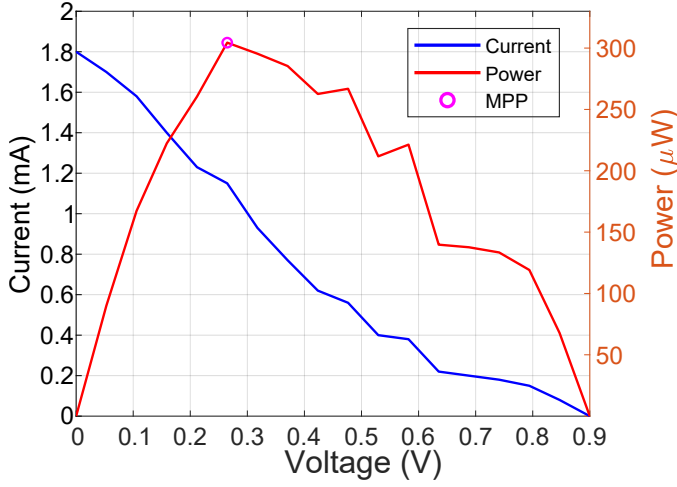
Fig. 8. The blue line is the cell's voltage vs. current characteristic, the red one represents the output power ($V \cdot I$) provided by th cell. The purple circle highlights the maximum power point (MPP) showing that it is approximately 35% of the open circuit voltage.

This frequency is $10\,\mathrm{kHz}$, which offers a good trade-off.

Due to this choice, in the following, a single value per impedance spectroscopy will be considered and reported in the presented plots. These measurements assessed the correlation among stem frequency, electrical impedance, and SWP. The set-up implemented to monitor stem frequency, stem electrical impedance, and SWP is described in section II. *Pearson's* correlation coefficient [31] was chosen as the parameter to assess this correlation.

We chose this parameter because of its well-known reliability in assessing correlation among different quantities and since our attention focused on quantities trends rather than their absolute value. Since plants are living beings, they are characterized by a significant variability of the absolute value of their parameters. Thus, observing quantities' behaviors over time rather than their instantaneous values leads to more meaningful information.

All the analyzed quantities (visible light intensity, air humidity, temperature, soil water potential, stem impedance phase, modulus, and stem frequency) were sampled once per hour, and the related time series underwent *Pearson's* correlation test.

highlighted that the impedance variations over time at higher frequencies are too small to indicate the plant's status. Therefore, since stem impedance was analyzed through wide-range spectroscopy, a single frequency was selected for the analysis.

Since the stem frequency was sampled once per hour, the time series were filtered before the correlation test with a moving average with a lag equal to 24. This focused on their
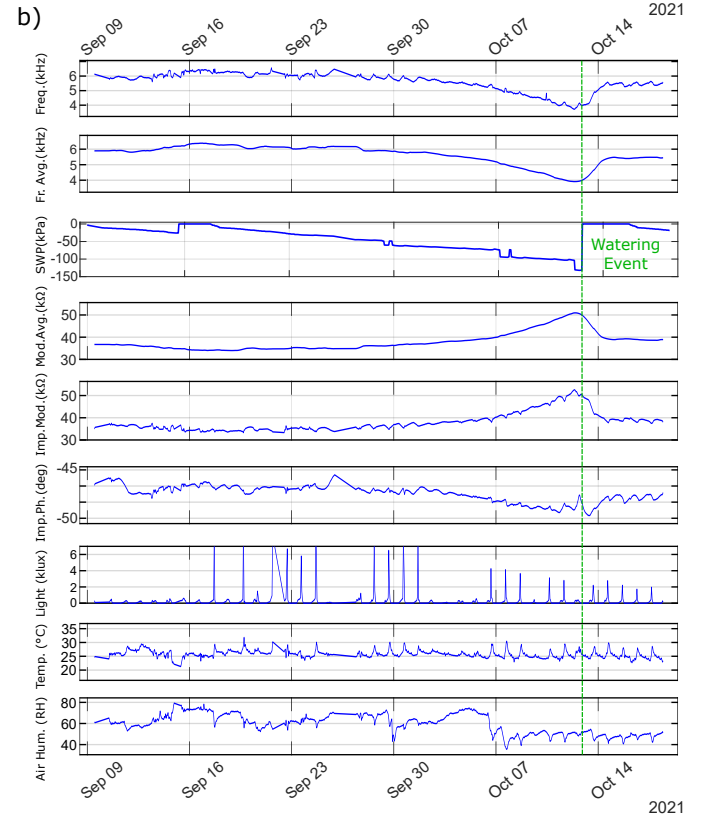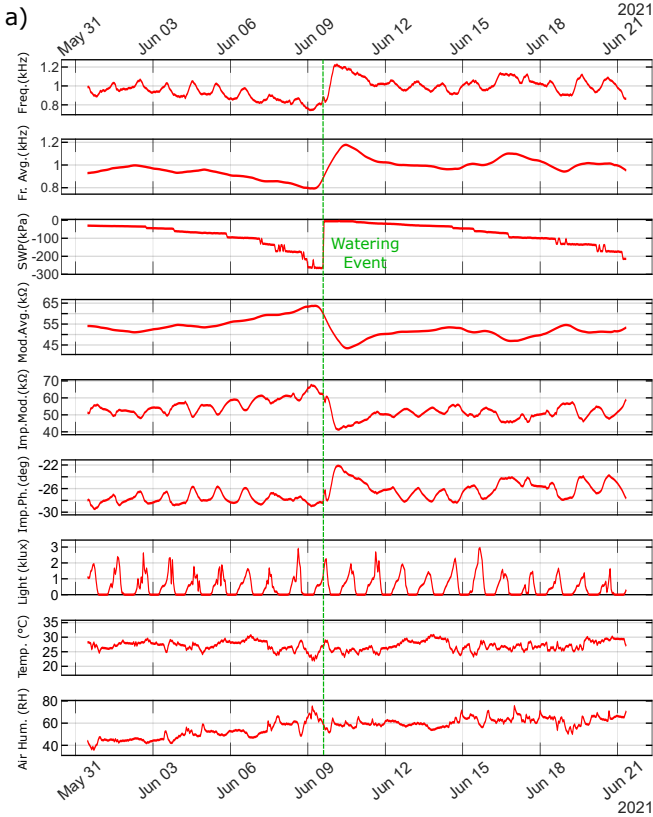

Fig. 9. a) Stem frequency, stem frequency moving average, soil water potential (SWP), stem impedance modulus moving average, stem impedance modulus, stem impedance, visible light intensity, ambient temperature, and air humidity phase for plant 1.
b) Stem frequency, stem frequency moving average, soil water potential (SWP), stem impedance modulus moving average, stem impedance modulus, stem impedance phase, visible light intensity, ambient temperature, and air humidity for plant 2. Both plants experience watering events, and the green vertical dashed line has highlighted them. Soil water potential measures are differential. Therefore, its value is assessed with respect to a known one. The reference value refers to thoroughly wet soil.

overall trend (dominated by soil water potential variation) rather than their short-term changes [17]. This statistical manipulation highlighted the long-term behavior, filtering out the stem frequency and daily impedance cycle (detailed below).

Tests were carried out on two plants grown in their pot in two different seasons (late spring and early autumn, Northern Hemisphere) to have reproducible results. Measurements are shown in figure 9.a and 9.b for plants 1 and 2, respectively.

As pointed out, the two plants show quite different stem frequency absolute values but had similar behaviors over time. Plant 1 stem frequency baseline values are lower than plant 2 ones. This explains the difference in the range of stem impedance modulus for the two plants. It can be easily noticed that in both cases, stem frequency and impedance modulus are inversely proportional.

Stem frequency and impedance modulus undergo an evident trend change after a watering event (frequency increase and impedance modulus decrease). This change in trend is easily noticeable in the stem frequency moving average. Therefore, this quantity was exploited to decide when to water both plants. Its development was constantly tracked, and plants were watered when its value reached a decrease of about 20% with respect to the one evaluated seven days before. Soil water potential levels corresponding to this decrease showed that both plants were subject to water stress. Stem frequency, impedance modulus, and phase showed a daily trend that led to a local stem frequency maximum during the daytime, a simultaneous stem impedance minimum, and an impedance phase local maximum. This behavior has already been observed in a previous study regarding tobacco stem electrical impedance monitoring [9]. In fact, *Garlando et al.* showed that impedance modulus decreases when light impinges on the plant. This variation may correlate to plants' photosynthetic activity that intensifies when enlightened. Quantities' daily trends are more noticeable in plant 1 than in plant 2.

Despite impedance phase and stem frequency seemed to have a good correlation in both cases (see table I), our attention focused on the relationship between impedance modulus and stem frequency. This choice was because the impedance modulus can be easily read with a simple electronic system, while the phase requires a more complex and power-consuming conditioning circuit. Therefore, stem frequency monitoring is a more feasible implementation for a "plant wearable system."

Statistical analyses have led to optimal *Pearson's* correlation coefficients (p-values) between stem frequency, stem impedance modulus, and soil water potential, all higher or equal to 0.75 (in absolute value). Statistical test results are reported in table I. They focused on the period close to the watering event (three days before and three after) to better disentangle soil water potential's impact on stem frequencies (and, thus, on stem impedance) from other parameters' contribution. Moreover, since a plant is a living being, its reaction to external stimuli (such as a watering event) has a certain delay with respect to the event that caused it. As highlighted in figure9, stem frequency does not react immediately to the watering event. Hence the choice of the period for statistical analysis.

Pearson's correlation test numerical results clearly show

	Stem Frequency	Impedance Modulus	Impedance Phase	Soil Water Potential
Stem Frequency	1 / 1	-0,99 / -0,99	0,92 / 0,89	0,85 / 0,76
Impedance Modulus	-0,99 / -0,99	1 / 1	-0,86 / -0,85	-0,90 / -0,75
Impedance Phase	0,92 / 0,89	-0,86 / -0,85	1 / 1	0,61 / 0,63
Soil Water Potential	0,85 / 0,76	-0,90 / -0,75	0,61 / 0,63	1 / 1

TABLE I
Pearson's CORRELATION COEFFICIENTS EVALUATED AMONG THE QUANTITIES REPORTED IN FIGURE 9. RED VALUES REFER TO PLANT 1, WHILE THE BLUE ONES TO PLANT 2.

that: soil water potential and stem impedance modulus are strictly correlated (correlation coefficients up to 0.9 in absolute value), stem frequency and impedance modulus are very strongly related (correlation coefficients equal to -0.99 for both plants), and, as expected, stem frequency and soil water potential are quite strictly correlated too. The values related to their time series are up to 0.85. This means that inspecting stem frequency provides reliable information about soil water potential and, therefore, about plants' watering stress.

B. Inter-Plant Communication

This experiment monitored stem frequency behavior over time by exploiting plant stem and soil electrical conductivity. The set-up has been detailed in section II. As stated, this analysis involved two plants growing in the same pot.

Together with the stem frequency, soil water potential (SWP) was monitored as a control parameter with the circuit described in section II, subsection *Intra- and Inter-Plant Communication*.

The measurements lasted over a month and a half, and plants were subject to water stress. Therefore, they were watered only when a visual evaluation suggested.

The plant's conditions before and after the watering event are depicted in figure 10.a and 10.c respectively. Figure 10.b shows stem frequency and SWP in the period close to the watering event. The whole data set showing the data acquired during the experiment is reported in figure 11.

As described in section II, the signal injection was performed on the plant under test (see figure1). Therefore, stem frequency depended only on this plant's water stress status.

This figure shows that frequency and soil water potential have a similar behavior since they increase and decrease almost simultaneously, as already noticeable in figure 9.a and 9.b. The delay between the occurrence of a watering event (pointed out by the dashed line and a sharp increase in SWP trend) is due to latency in the plant's response to environmental parameters change. Frequency and soil water potential trends similarity is particularly noticeable in the green line in figure11, upper plot (raw data polynomial interpolation). In fact, before the watering event, they decrease, rise after, and decrease again when the soil dries.

Moreover, the red line (raw data) shows the same daily cycle as the plants in figure 9.a and 9.b leading to local minima and maxima that repeat daily.
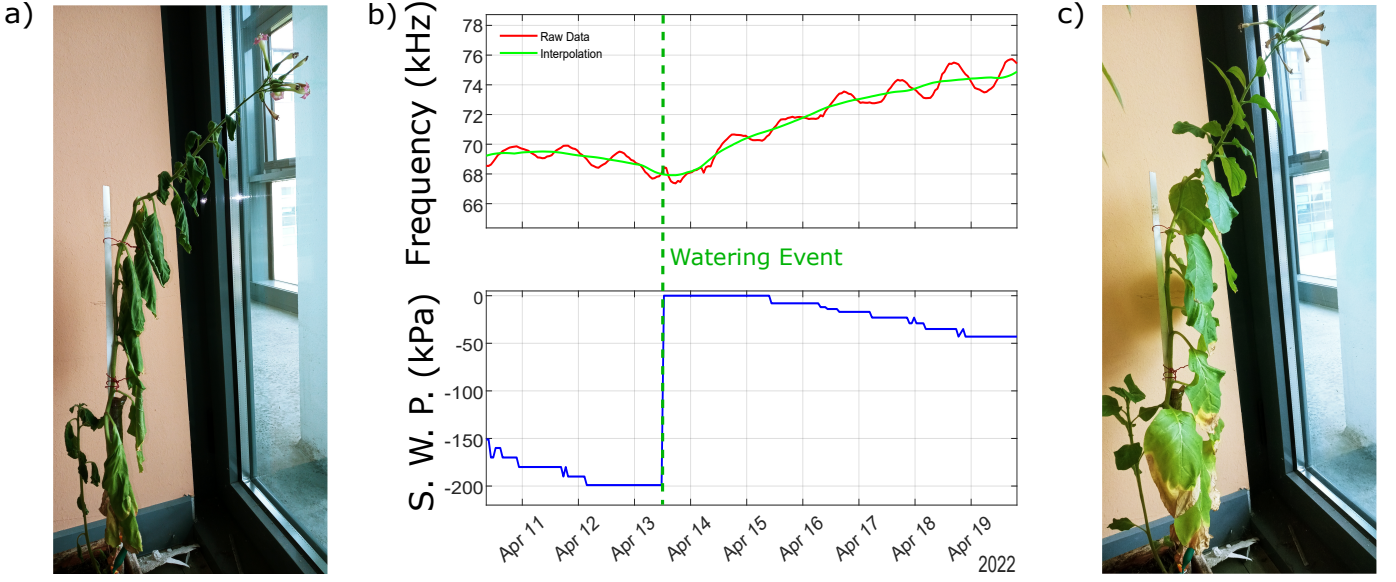
Fig. 10. a) Plant under test on April 13*th* before the watering event. This condition was considered dried enough. Therefore water was provided to the plant on the same day, as highlighted by the dashed vertical line. b) Frequency and Soil Water Potential trends around the watering event. c) Plant under test on April 19*th*.
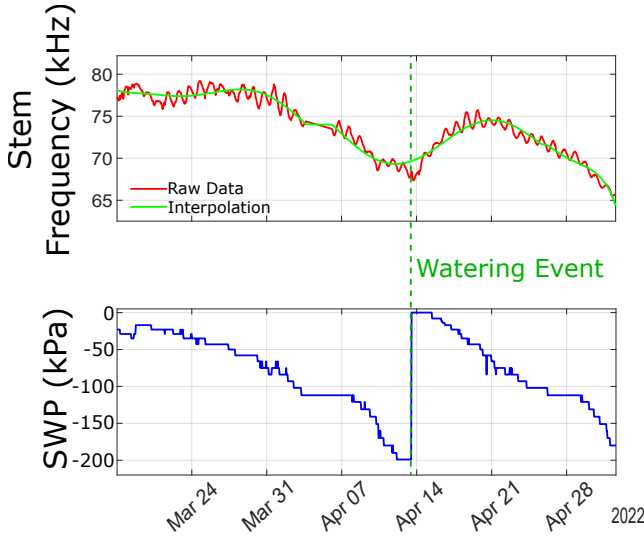

Fig. 11. The graph on the top shows the frequency values read by the receiving system during the analyses. The red line represents raw data, while the green one is a 5th degree polynomial interpolation. The bottom graph reports the soil water potential values over time. The dark green vertical dashed lines show the occurred watering event. Stem frequencies and SWP were evaluated with an MCU whose clock was set to $1\,\mathrm{MHz}$. Therefore, neglecting clock frequency shift, stem frequencies were read with a relative error lower than 8%, while SWP with an error lower than 2%.

Performed tests, presented in figure 11, lasted several weeks without showing failures and demonstrated that the harvested and stored power was always sufficient. This suggested that the implemented power management strategies and devices (i.e., energy harvesting and storing) were effective enough to provide reliability to the complete system.

IV. CONCLUSION

In this paper, we demonstrated how it is possible to directly monitor plant watering stress status by stem electrical impedance analysis. This physical quantity has been measured with a straightforward and reliable method, with devices installed directly on the plant, measuring the frequency of a square wave directly correlated to the impedance. The strong correlation between plant water stress status and frequency was proved with experiments.

Furthermore, a single reading system connected to a plant reads data coming from multiple sources. A neighboring plant water stress status and a sensor placed in the soil were monitored from the same device without wired connections.

The system was completely autonomous from the energy point of view. Two different energy sources were exploited, and no batteries were used in the set-up. Being the system battery-less (a critical feature for systems meant to be installed outdoors) and entirely based on simple, off-the-shelf, compact electronic components, we demonstrated that it could be easily deployed into the fields.

Experiments proved that plants' branches, leaves, roots, and soil can be exploited as communication channels for electrical signals' propagation. This feature may be exploited in future applications toward the realization of the so-called *Internet of Plants*: a network where nodes are the plants themselves because, as we demonstrated, the transmission of data and the monitoring of plant's health can be done in parallel, allowing both functionalities with a single transmission. The plan is to modulate the transmitted signals and exchange information among plants in future developments. Moreover, signal propagation in different soils will be inspected. This will include different soil compositions and conditions. Moreover, further inspections will be conducted regarding the signal reconstruction circuitry (threshold voltage comparator) and its reliability.

REFERENCES

[1] A. L. Burrell, J. P. Evans, and M. G. De Kauwe, "Anthropogenic climate change has driven over 5 million km2 of drylands towards desertification.," *Nature Communications*, vol. 11, 1 2020. DOI: 10 . 1038 / s41467-020-17710-7. [Online]. Available: https://doi.org/10.1038/s41467-020-17710-7.

[2] European Environment Agency, "Soil degradation - environment in eu at the turn of the century (chapter 3.6)," 2020, Available Online (Last Modified 23 Nov 2020). [Online]. Available: https://www.eea.europa.eu/publications/92-9157-202-0/page306.html.

[3] A. Mahato, "Climate change and its impact on agriculture," *International Journal of Scientific and Research Publications*, vol. 4, no. 4, pp. 1–6, 2014.

[4] H. Ritchie and M. Roser, "Environmental impacts of food production," *Our World in Data*, 2020, https://ourworldindata.org/environmental-impacts-of-food.

[5] M. Roser, "Future population growth," *Our World in Data*, 2013, https://ourworldindata.org/future-population-growth.

[6] S. Tenzin, S. Siyang, T. Pobkrut, and T. Kerdcharoen, "Low cost weather station for climate-smart agriculture," in *2017 9th International Conference on Knowledge and Smart Technology (KST)*, 2017, pp. 172–177. DOI: 10.1109/KST.2017.7886085.

[7] T. Kasama, T. Koide, W. P. Bula, Y. Yaji, Y. Endo, and R. Miyake, "Low cost and robust field-deployable environmental sensor for smart agriculture," in *2019 2nd International Symposium on Devices, Circuits and Systems (ISDCS)*, IEEE, 2019, pp. 1–4.

[8] C. Nakayama, T. Katumata, H. Aizawa, S. Komuro, and H. Arima, "Two dimensional evaluation of soil property for agriculture," in *2008 International Conference on Smart Manufacturing Application*, 2008, pp. 142–145. DOI: 10.1109/ICSMA.2008.4505629. [Online]. Available: https://ieeexplore.ieee.org/document/4505629.

[9] U. Garlando, S. Calvo, M. Barezzi, A. Sanginario, P. Motto Ros, and D. Demarchi, "Ask the plants directly: Understanding plant needs using electrical impedance measurements," *Computers and Electronics in Agriculture*, vol. 193, p. 106 707, 2022, ISSN: 0168-1699. DOI: https : / / doi . org / 10 . 1016 / j . compag . 2022 . 106707. [Online]. Available: https : / / www . sciencedirect . com / science/article/pii/S0168169922000242.

[10] V. Palazzari, P. Mezzanotte, F. Alimenti, *et al.*, "Leaf compatible "eco-friendly" temperature sensor clip for high density monitoring wireless networks," in *2015 IEEE 15th Mediterranean Microwave Symposium (MMS)*, 2015, pp. 1–4. DOI: 10 . 1109 / MMS . 2015 . 7375456.

[11] E. Pievanelli, R. Stefanelli, and D. Trinchero, "Microwave-based leaf wetness detection in agricultural wireless sensor networks," in *2016 IEEE Sensors Applications Symposium (SAS)*, IEEE, 2016, pp. 1–4.

[12] P. Pipitsunthonsan, J. Sopharat, P. Sirisuk, and M. Chongcheawchamnan, "Leaf sensor for stomata transpiration monitoring using temperature and humidity," in *2018 21st International Symposium on Wireless Personal Multimedia Communications (WPMC)*, IEEE, 2018, pp. 252–255.

[13] S. N. Daskalakis, G. Goussetis, S. D. Assimonis, M. M. Tentzeris, and A. Georgiadis, "A uw backscatter-morse-leaf sensor for low-power agricultural wireless sensor networks," *IEEE Sensors Journal*, vol. 18, no. 19, pp. 7889–7898, 2018. DOI: 10 . 1109 / JSEN . 2018 . 2861431.

[14] Y. Zhao, S. Gao, J. Zhu, *et al.*, "Multifunctional stretchable sensors for continuous monitoring of long-term leaf physiology and microclimate," *ACS omega*, vol. 4, no. 5, pp. 9522–9530, 2019.

[15] D. Lo Presti, S. Cimini, C. Massaroni, *et al.*, "Plant wearable sensors based on fbg technology for growth and microclimate monitoring," *Sensors*, vol. 21, no. 19, p. 6327, 2021.

[16] D. Tran, F. Dutoit, E. Najdenovska, *et al.*, "Electrophysiological assessment of plant status outside a faraday cage using supervised machine learning," *Scientific reports*, vol. 9, no. 1, p. 17 073, 2019.

[17] U. Garlando, L. Bar-On, P. M. Ros, *et al.*, "Analysis of in vivo plant stem impedance variations in relation with external conditions daily cycle," in *2021 IEEE International Symposium on Circuits and Systems (ISCAS)*, 2021, pp. 1–5. DOI: 10.1109/ISCAS51556.2021.9401242.

[18] U. Garlando, L. Bar-On, P. M. Ros, *et al.*, "Towards optimal green plant irrigation: Watering and body electrical impedance," Cited by: 6, vol. 2020-October, 2020. [Online]. Available: https://www.scopus.com/inward/record.uri?eid=2-s2.0-85109017326&partnerID=40&md5=a7b7115c8dc7e56a569fab7d73ec4f0f.

[19] D. Corwin and S. M. Lesch, "Application of soil electrical conductivity to precision agriculture: Theory, principles, and guidelines," *Agronomy journal*, vol. 95, no. 3, pp. 455–471, 2003.

[20] P. M. Ros, E. Macrelli, A. Sanginario, Y. Shacham-Diamand, and D. Demarchi, "Electronic system for signal transmission inside green plant body," in *2019 IEEE International Symposium on Circuits and Systems (ISCAS)*, 2019, pp. 1–5. DOI: 10.1109/ISCAS.2019.8702577.

[21] P. Dasgupta, B. S. Das, and S. K. Sen, "Soil water potential and recoverable water stress in drought tolerant and susceptible rice varieties," *Agricultural Water Management*, vol. 152, pp. 110–118, 2015, ISSN: 0378-3774. DOI: https://doi.org/10.1016/j.agwat.2014.12.013. [Online]. Available: https : / / www . sciencedirect . com / science/article/pii/S0378377414003990.

[22] J. Yang, K. Liu, Z. Wang, Y. Du, and J. Zhang, "Water-saving and high-yielding irrigation for lowland rice by controlling limiting values of soil water potential," *Journal of Integrative Plant Biology*, vol. 49, no. 10, pp. 1445–1454, 2007.

[23] J. Janesch, "Two-wire vs. four-wire resistance measurements: Which configuration makes sense for your application?" *Keithley Instruments, Inc.*, 2013.

[24] R. Aloni, "Vascular differentiation within the plant," in *Vascular Differentiation and Plant Growth Regulators*. Berlin, Heidelberg: Springer Berlin Heidelberg, 1988, pp. 39–62, ISBN: 978-3-642-73446-5. DOI: 10.1007/978-3-642-73446-5_3. [Online]. Available: https://doi.org/10.1007/978-3-642-73446-5_3.

[25] L. Bar-On, U. Garlando, M. Sophocleous, *et al.*, "Electrical modelling of in-vivo impedance spectroscopy of nicotiana tabacum plants," *Frontiers in Electronics*, vol. 2, p. 14, 2021, ISSN: 2673-5857. DOI: 10.3389/felec.2021.753145. [Online]. Available: https://www.frontiersin.org/article/10.3389/felec.2021.753145.

[26] Z. G. Datsios, P. N. Mikropoulos, and I. Karakousis, "Laboratory characterization and modeling of dc electrical resistivity of sandy soil with variable water resistivity and content," *IEEE Transactions on Dielectrics and Electrical Insulation*, vol. 24, no. 5, pp. 3063–3072, 2017. DOI: 10.1109/TDEI.2017.006583.

[27] C. Ma, J. Li, and S. Yu, "Method of soil electrical conductivity measurement based on multi-sensor data fusion," in *2011 International Conference on Mechatronic Science, Electric Engineering and Computer (MEC)*, 2011, pp. 1219–1221. DOI: 10.1109/MEC.2011.6025686.

[28] A. Castillo-Atoche, J. Vázquez-Castillo, E. Osorio-de-la-Rosa, *et al.*, "An energy-saving data statistics-driven management technique for bio-powered indoor wireless sensor nodes," *IEEE Transactions on Instrumentation and Measurement*, vol. 70, pp. 1–10, 2021. DOI: 10.1109/TIM.2021.3063187.

[29] E. Osorio de la Rosa, J. Vázquez Castillo, M. Carmona Campos, *et al.*, "Plant microbial fuel cells–based energy harvester system for self-powered iot applications," *Sensors*, vol. 19, no. 6, 2019, ISSN: 1424-8220. DOI: 10.3390/s19061378. [Online]. Available: https://www.mdpi.com/1424-8220/19/6/1378.

[30] M. Barezzi, U. Garlando, F. Pettiti, *et al.*, "Long-range low-power soil water content monitoring system for precision agriculture," in *2022 IEEE 13th Latin America Symposium on Circuits and System (LASCAS)*, 2022, pp. 1–4. DOI: 10.1109/LASCAS53948.2022.9789070.

[31] A. Garcia Asuero, A. Sayago, and G. González, "The correlation coefficient: An overview," *Critical Reviews in Analytical Chemistry - CRIT REV ANAL CHEM*, vol. 36, pp. 41–59, Jan. 2006. DOI: 10.1080/10408340500526766.

Umberto Garlando (Member IEEE) received both his bachelor's and master's degrees in electronic engineering, at Politecnico di Torino, in 2013 and 2015, respectively. From 2016 to 2019, he pursued a Ph.D. in electronic engineering at the VLSILab of Politecnico di Torino, working on CAD and EDA tools for FCN (Field coupled nanocomputing). He worked in the development of the ToPoliNano framework, focusing on the simulation part. In 2020, he joined the MiNES (Micro and Nano Electronic Systems) group as a research associate, where he works on a fast-growing field such as the smart-systems for agri-food technology.

Stefano Calvo has obtained both his degrees at Politecnico di Torino. Bachelor's in Physical Engeneering in 2018 and Master's degree in Nanotechnlogies for ICTs in 2020. In his Master's degree thesis he developed an energetically autonomous system for measuring the impedance of the stem of plants. He is currently doing his Ph.D. at the Politecnico di Torino.

Mattia Barezzi has obtained his bachelor's degree in Information Engineering at University of Parma in 2017 and he is currently working on his master's thesis in Electronic Engineering at Politecnico di Torino developing an autonomous low-power electronic system able to send useful data sampled from environmental and soil sensors via LoRa communication radio protocol.

Alessandro Sanginario (MemberIEEE) received a degree in Biomedical Engineering and a Ph.D. degree in Physics from the Politecnico di Torino, Italy, in 2006 and 2010, respectively. In 2009, he was a Visiting Scholar with University of South-Eastern Norway. After the Ph.D., he held a postdoctoral position at the Chilab Laboratory, Electronics Department at Politecnico di Torino and, then, at the Istituto Italiano di Tecnologia (IIT)@PoliTo Center for Space Human Robotics until 2017. He is currently working as a researcher with the MiNES (Micro and Nano Electronic Systems) Laboratory, Politecnico di Torino and researcher technician with the Department of Electronics and Telecommunications of Politecnico di Torino. His studies concern MEMS and advanced sensors, especially for biomedical applications, micro- and nano- system integration and electronics. He is the author and co-author of two patents and more than 60 scientific publications in journals and conference proceedings related to electronics, biomedical engineering and MEMS.

Paolo Motto Ros (Member, IEEE) is Senior Post-Doctoral Researcher and Adjunct Professor at Politecnico di Torino (Torino, Italy), Dipartimento di Elettronica e Telecomunicazioni, with the MiNES (Micro&Nano Electronic Systems) group. He received the electronic engineering degree and the Ph.D. in electronic engineering from the Politecnico di Torino, Torino, Italy, in 2005 and 2009, respectively. From 2009 to 2012 he was with Neuronica Laboratory (Dipartimento di Elettronica, Politecnico di Torino) as post-doc researcher (jointly with, 2006-2011, Istituto Nazionale Fisica Nucleare, INFN, Italy). From 2012 to 2019 he was with Istituto Italiano di Tecnologia (Center for Space Human Robotics, CSHR, Torino, Italy, and, since 2016, Electronic Design Laboratory, EDL, Genova, Italy) as senior (since 2014) post-doc researcher. He joined the Politecnico di Torino, Dipartimento di Elettronica e Telecomunicazioni, in 2019. He was member of the organizing staff of the IEEE BioCAS 2017 conference, and member of the organizing committee of the IEEE ICECS 2019 conference and the FoodCAS Satellite Event at the ISCAS 2021 conference. He is guest editor of MDPI Sensors and topic editor of Frontiers in Neurorobotics. He counts more than 60 publications; current research interests include: event-driven digital integrated circuits, architectures, and systems; low-power smart sensor networks; bio-inspired electronics; biomedical and humanoid robotic applications.

Danilo Demarchi (Senior Member, IEEE) received the Engineering and Ph.D. degrees in electronics engineering from Politecnico di Torino, Torino, Italy, in 1991 and 1995, respectively. Associate Professor with Politecnico di Torino, Department of Electronics and Telecommunications. Lecturer at EPFL Lausanne and Visiting Professor at Tel Aviv University. In 2018, he has been Visiting Scientist at MIT and Harvard Medical School. He has authored and coauthored 5 patents and more than 250 scientific publications in international journals and peer-reviewed conference proceedings. He is leading the MiNES (Micro&Nano Electronic Systems, http://mines.polito.it) Laboratory of Politecnico di Torino. Prof. Demarchi is member of the IEEE Sensors Council and of the BioCAS Technical Committee, Associate Editor for the IEEE SENSORS and of the Springer Journal BioNanoScience, General Chair of Biomedical Circuits and Systems Conference edition in Torino, October 2017, and Founder of IEEE FoodCAS Workshop (Circuits and Systems for the Food Chain).